Inorg. Chem. **2007**, *46*, 9294–9302

Enhancement in Electronic Communication upon Replacement of Mo–O by Mo–S Bonds in Tetranuclear Clusters of the Type $[Mo_2]_2(\mu\text{-E–E})_2$ (E = O or S)

F. Albert Cotton,[†,‡] Zhong Li,[‡] Chun Y. Liu,*[,‡,§] and Carlos A. Murillo*[,‡]

Department of Chemistry and Laboratory for Molecular Structure and Bonding, P.O. Box 3012, Texas A&M University, College Station, Texas 77842-3012, and Department of Chemistry, Tongji University, Shanghai 200092, People's Republic of China

Received July 2, 2007

A tetranuclear cluster containing two quadruply bonded *cis*-$Mo_2(DAniF)_2$ units (DAniF = *N*,*N*′-di-*p*-anisylformamidinate) linked by four hydroxide groups (**1**) was obtained by hydrolysis of $[Mo_2(cis\text{-}DAniF)_2](\mu\text{-}OCH_3)_4$. Analogous compounds linked by two bidentate bridges (*o*-$O_2C_6H_4$ for **2**, *o*-$O_2C_{10}H_6$ for **3**, and *o*-$S_2C_6H_4$ for **4**) were synthesized by direct assembly of the corner species precursor $[Mo_2(cis\text{-}DAniF)_2(NCCH_3)_4](BF_4)_2$ and the respective protonated ligands. All four compounds were characterized by X-ray crystallography. Cyclic voltammograms of the O-linked compound **2** and the S analogue **4** show two reversible one-electron-oxidation processes with potential separations ($\Delta E_{1/2}$) of 474 and 776 mV, respectively. The large increase of about 300 mV in $\Delta E_{1/2}$ for the S analogue relative to that of the O compound is consistent with a large increase in electronic communication. This enhancement occurs despite the increase of ca. 0.45 Å in nonbonding separation between the midpoints of the Mo_2 units, which changes from 3.266 Å in **2** to 3.72 Å in **4**, and the increase of ca. 0.4 Å in M–E distances as E changes from O to S. Density functional theory calculations show that the increase in electronic communication between the metal centers in **4** is due to a superexchange pathway involving d and p orbitals in the linker E atoms that is less important in **2**.

Introduction

Electronic communication between two chemical entities mediated by linkers is a process of fundamental importance in chemistry, and electron-transfer processes have been studied in many key areas of chemistry and biological systems ranging from simple redox reactions to photosynthesis and enzymatic processes.[1] The most intensely studied systems are those containing two single-metal centers linked by an organic moiety as epitomized by the pyrazine (pyz)-bridged diruthenium complex, $[Ru(NH_3)_5]pyz[Ru(NH_3)_5]^{5+}$, prepared by Creutz and Taube in the late 1960s.[2] A key aspect pertaining to this and other compounds having two bridged metal centers is the analysis of how the two metal units communicate via the linker and the nature of the pathway for electrons moving between metal centers.[3] It has been known that an important electron pathway for complexes with conjugated linkers is through metal-to-ligand back-π-bonding interactions such as $d-\pi^*$, which are often found in species containing two linked single-metal[4] units, but others such as superexchange and direct ligand orbital overlap have also been suggested.[5]

* To whom correspondence should be addressed. E-mail: cyliu06@mail.tongji.edu.cn (C.Y.L.), murillo@tamu.edu (C.A.M.).
† Deceased February 20, 2007.
‡ Texas A&M University.
§ Tongji University.

(1) (a) Brunschwig, B. S.; Sutin, N. *Coord. Chem. Rev.* **1999**, *187*, 233. (b) Holm, R. H.; Kennepohl, P.; Solomon, E. I. *Chem. Rev.* **1996**, *96*, 2239. (c) Marcus, R. A. *J. Electroanal. Chem.* **1997**, *438*, 251. (d) Cameron, C. G.; Pickup, P. G. *J. Am. Chem. Soc.* **1999**, *121*, 7710. (e) Demadis, K. D.; Hartshorn, C. M.; Meyer, T. J. *Chem. Rev.* **2001**, *101*, 2655. (f) Lau, V. C.; Berben, L. A.; Long, J. R. *J. Am. Chem. Soc.* **2002**, *124*, 9042. (g) Shi, Y.; Yee, G. T.; Wang, G.; Ren, T. *J. Am. Chem. Soc.* **2004**, *126*, 10552.

(2) Creutz, C.; Taube, H. *J. Am. Chem. Soc.* **1969**, *91*, 3988. (b) Creutz, C.; Taube, H. *J. Am. Chem. Soc.* **1973**, *95*, 1086.

(3) For example, see: (a) Creutz, C. *Prog. Inorg. Chem.* **1983**, *30*, 1. (b) Richardson, D. E.; Taube, H. *Coord. Chem. Rev.* **1984**, *60*, 107. (c) Demadis, K. D.; Hartshorn, C. M.; Meyer, T. J. *Chem. Rev.* **2001**, *101*, 2655. (d) Joshi, H. K.; Cooney, J. J. A.; Inscore, F. E.; Gruhn, N. E.; Lichtenberger, D. L.; Enemark, J. H. *Proc. Natl. Acad. Sci. U.S.A.* **2003**, *100*, 3719.

(4) For example, see: Bencini, A.; Ciofini, I.; Daul, C. A.; Ferretti, A. *J. Am. Chem. Soc.* **1999**, *121*, 11418.

(5) (a) Crutchley, R. J. *Adv. Inorg. Chem.* **1994**, *41*, 273. (b) Dinolfo, P. H.; Wiliams, M. E.; Stern, C. L.; Hupp, J. T. *J. Am. Chem. Soc.* **2004**, *126*, 12989.

10.1021/ic701303k CCC: $37.00
Published on Web 10/02/2007

Scheme 1

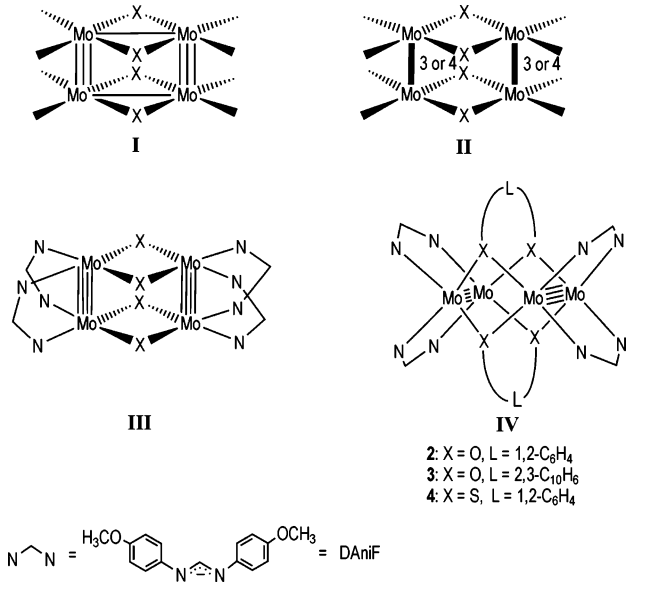

Lately there have been efforts to probe electronic communication using dimetal units instead of single-metal atom units.[6] In some aspects, these systems resemble those with single-metal atoms, but in others, they provide significant advantages because they offer additional structural and spectroscopic probes. It has been shown that similar to compounds with single-metal units, the communication is enhanced when linkers possess conjugated systems instead of saturated structures.[7] Furthermore, in compounds of the type $[(DAniF)_3Mo_2]_2(\mu\text{-}O_2C(CH{=}CH)_nCO_2]$, where $n = 0{-}4$ and DAniF = *N*,*N*′-di-*p*-anisylformamidinate, communication diminishes as the separation between Mo_2 units increases.[7a,b] However, it is now well-established that a pathway not available to species with single-metal atoms, namely, one that uses $\delta{-}\pi^*$ interactions, is crucial when covalently bonded dimetal units are present.[7a,8]

Recently, cyclic tetranuclear compounds consisting of two covalently bonded Mo_2 units joined by four single-atom bridging ligands have been investigated.[6c,9] Such compounds are sometimes referred to as cuboidal or rectangular Mo_4 clusters because the four Mo atoms from the two Mo_2 units lie on a plane defining a rectangle. There are three important types, **I**−**III**, which have a common Mo_4X_4 core (Scheme 1). Type **I** clusters have two triply bonded Mo_2 units joined by two Mo−Mo single bonds. They are formed by a [2 + 2] cycloaddition that involves breaking of the δ bonds of two quadruply bonded Mo_2 units followed by the formation of two single bonds between the triply bonded dimetal units. For halogen-bridged complexes of the type $Mo_4X_8L_4$ (X = Cl, Br, and I; L = $P(OMe_3)_3$, PEt_3), only the chloro complex can be assigned unambiguously to type **I** according to single-crystal X-ray analysis,[10,11] while in the iodide analogue,[12] the quadruple bonds remain intact and thus it is assigned to type **II**.

Scheme 2

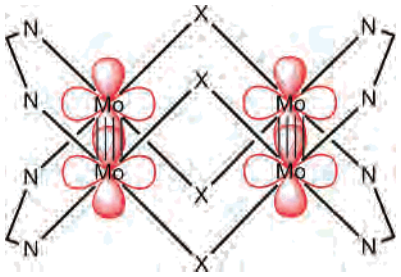

An intermediate situation is observed in compounds of the type $[Mo_2(cis\text{-}DAniF)_2]_2(\mu\text{-}X_4)$, where DAniF = *N*,*N*′-di-*p*-anisylformamidinate and X = Cl,[13] Br, I,[14] OMe, or OEt.[15] These compounds show two successive one-electron oxidation processes. For the halides (X = Cl, Br, and I), the electronic coupling, determined from the separation between redox potentials ($\Delta E_{1/2}$), is linearly related to the atomic size of X, which also controls the metal−metal nonbonding separation.[14] $\Delta E_{1/2}$ varies from 540 mV for the chloride-bridged compound to 440 mV for the iodide analogue. For these compounds and also for the alkoxides, it was shown that electron removal from the quadruply bonded Mo_2 units strengthens the orbital interactions and a transition from nonbonding to bonding interaction has been observed as the oxidation number increases in compounds such as $\{[Mo_2(cis\text{-}DAniF)_2]_2(\mu\text{-}OCH_3)_4\}^{n+}$ ($n = 0$, 1, and 2).[15] This is possible because of the idealized D_{2h} symmetry of these compounds that orient the δ orbitals from the Mo_2 units in such a way that allow direct metal−metal interactions when the separation between Mo_2 units is short (Scheme 2).

Very recently, there have been two reports indicating that by replacement of O by S atoms in certain linkers, there is an increase in electronic communication between dimetal units.[16] We have explored further this effect and now report three new compounds having O donor atoms, $[Mo_2(cis\text{-}DAniF)_2]_2(\mu\text{-}OH)_4$ (**1**), $[Mo_2(cis\text{-}DAniF)_2]_2[\mu\text{-}(o\text{-}O_2C_6H_4)_2]$ (**2**), and $[Mo_2(cis\text{-}DAniF)_2]_2[\mu\text{-}(o\text{-}O_2C_{10}H_6)_2]$ (**3**), and the S

(6) For example, see: (a) Ren, T. *Organometallics* **2005**, *24*, 4854. (b) Xu, G. L.; Zou, G.; Ni, Y. H.; DeRosa, M. C.; Crutcheley, R. J.; Ren, T. *J. Am. Chem. Soc.* **2003**, *125*, 10057. (c) Chisholm, M. H.; Macintosh, A. M. *Chem. Rev.* **2005**, *105*, 2949. (d) Cotton, F. A.; Lin, C.; Murillo, C. A. *Acc. Chem. Res.* **2001**, *34*, 759. (e) Cotton, F. A.; Lin, C.; Murillo, C. A. *Proc. Natl. Acad. Sci. U.S.A.* **2002**, *99*, 4810. (f) Chisholm, M. H.; Patmore, N. J. *Acc. Chem. Res.* **2007**, *40*, 19. (g) Bursten, B. E.; Chisholm, M. H.; D'Acchioli, J. S. *Inorg. Chem.* **2005**, *44*, 5571.

(7) (a) Cotton, F. A.; Donahue, J. P.; Murillo, C. A.; Pérez, L. M. *J. Am. Chem. Soc.* **2003**, *125*, 5486. (b) Cotton, F. A.; Donahue, J. P.; Murillo, C. A. *J. Am. Chem. Soc.* **2003**, *125*, 5436. (c) Cotton, F. A.; de Meijere, A.; Murillo, C. A.; Rauch, R.; Yu, R. *Polyhedron* **2006**, *25*, 219.

(8) Cotton, F. A.; Liu, C. Y.; Murillo, C. A.; Villagrán, D.; Wang, X. *J. Am. Chem. Soc.* **2004**, *126*, 14822.

(9) Cotton, F. A.; Daniels, L. M.; Guimet, I.; Henning, R. W.; Jordan, G. T.; Lin, C.; Murillo, C. A.; Schultz, A. J. *J. Am. Chem. Soc.* **1998**, *120*, 12531.

(10) McGinnis, R. N.; Ryan, T. R.; McCarley, R. E. *J. Am. Chem. Soc.* **1978**, *100*, 7900.

(11) Cotton, F. A.; Powell, G. L. *Inorg. Chem.* **1983**, *22*, 871.

(12) Ryan, T. R.; McCarley, R. E. *Inorg. Chem.* **1982**, *21*, 2072.

(13) Cotton, F. A.; Liu, C. Y.; Murillo, C. A.; Wang, X. *Chem. Commun.* **2003**, 2190.

(14) Cotton, F. A.; Liu, C. Y.; Murillo, C. A.; Zhao, Q. *Inorg. Chem.* **2006**, *45*, 9493.

(15) Cotton, F. A.; Li, Z.; Liu, C. Y.; Murillo, C. A.; Zhao, Q. *Inorg. Chem.* **2006**, *45*, 6387.

(16) (a) Chisholm, M. H.; Patmore, N. *Dalton Trans.* **2006**, 3164. (b) Cotton, F. A.; Li, Z.; Liu, C. Y.; Murillo, C. A. *Inorg. Chem.* **2007**, *46*, 7840.

analogue $[Mo_2(cis\text{-}DAniF)_2]_2[\mu\text{-}(o\text{-}S_2C_6H_4)_2]$ (**4**). While the four bridging atoms in all previously reported cuboidal clusters are isolated groups such as halides or alkoxides, in compounds **2**−**4**, the four bridging atoms are provided by only two bidentate ligands that bring together two Mo_2 units and represent a new subgroup of Mo_4 clusters (type **IV** in Scheme 1). In addition, the use of the S-containing linker $o\text{-}S_2C_6H_4$ generates a compound (**4**) that shows an exceptionally large potential separation ($\Delta E_{1/2}$ = 776 mV) when compared to that for the O-bridged analogue (**2**), for which this value is only 474 mV. This increase in the potential separation occurs even though the former has a $Mo_2\cdots Mo_2$ distance of 3.724 Å, considerably larger than that of 3.267 Å for **3**. Theoretical calculations at the density functional theory (DFT) level suggest that the large difference between **2** and **4** is due to the availability of a superexchange pathway in **4** that is not accessible in **2**.

Experimental Section

Materials and Methods. All reactions and manipulations were performed under a N_2 atmosphere, using either drybox or standard Schlenk-line techniques. Solvents were purified under Ar using a Glass Contour solvent purification system or distilled over appropriate drying agents under N_2. The corner piece precursor $[Mo_2(cis\text{-}DAniF)_2(NCCH_3)_4](BF_4)_2$ was prepared as reported.[17] The ligand precursors (a) pyrocatechol, (b) 2,3-dihydroxynaphthalene, and (c) benzene-1,2-dithiol were purchased from Aldrich and used as received.

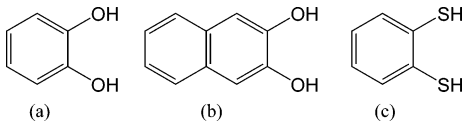

Physical and Spectroscopic Measurements. Elemental analyses were performed by Robertson Microlit Laboratories, Madison, NJ. Electronic spectra were measured on a Shimadzu UV-2501PC spectrometer in CH_2Cl_2 solutions. ^{1}H NMR spectra were recorded on an Inova-300 NMR spectrometer using $CDCl_3$ as the solvent. Cyclic voltammograms (CVs) and differential pulse voltammograms (DPVs) were collected in CH_2Cl_2 on a CH Instruments electrochemical analyzer equipped with Pt working and auxiliary electrodes and a Ag/AgCl reference electrode and using a scan rate (for CV) of 100 mV·s^{-1} and 0.10 M Bu_4NPF_6 as the electrolyte.

Preparation of $[Mo_2(cis\text{-}DAniF)_2]_2(\mu\text{-}OH)_4$ (1). To a solution of $[Mo_2(cis\text{-}DAniF)_2(NCCH_3)_4](BF_4)_2$ (208 mg, 0.200 mmol) in 20 mL of tetrahydrofuran (THF) was added slowly and with stirring 2.0 mL of a 0.50 M solution of $NaOCH_3$ in methanol. The color of the mixture changed from red to brown. After the reaction mixture was stirred for 1 h, the solvent was removed under vacuum. The residue was extracted with CH_2Cl_2 (3 × 5 mL), and the combined extracts were filtered through a Celite-packed frit. After removal of the solvent from the solution, the solid was dissolved in 15 mL of THF. A layer of O_2-free water was then added to the brown solution. Red block crystals formed within 2 weeks. Yield: 60 mg (41%). ^{1}H NMR (δ, ppm in $CDCl_3$): 8.67 (s, 4 H, −NC*H*N−), 6.63 (d, 16 H, aromatic C−*H*), 6.49 (d, 16 H, aromatic C−*H*), 3.17 (s, 24 H, −CH_3 in DAniF), 2.25 (s, 4 H, −O*H*). UV−vis [λ_{max}, nm (ϵ, M^{-1}·mol^{-1})]: 450 (1.4 × 10^3). Anal. Calcd for $C_{60}H_{70}Mo_4N_8O_{15}$ (**2**·3H_2O): C, 46.94; H, 4.56; N, 7.31. Found: C, 46.76; H, 4.12; N, 7.72.

Preparation of $[Mo_2(cis\text{-}DAniF)_2]_2[(\mu\text{-}o\text{-}O_2C_6H_4)_2]$ (2). To a Schlenk flask containing a mixture of $[Mo_2(cis\text{-}DAniF)_2(NCCH_3)_4](BF_4)_2$ (208 mg, 0.200 mmol) and pyrocatechol (22 mg, 0.20 mmol) was added 20 mL of ethanol. A brown precipitate formed immediately. The reaction mixture was stirred at ambient temperature for 1 h. After the supernatant solution was decanted, the remaining solid was washed with ethanol (2 × 15 mL) and then dried under vacuum. The solid was dissolved in 15 mL of dichloromethane. After the mixture was passed through a Celite-packed frit, the filtrate was layered with hexanes. Red-brown crystals were collected after 7 days. Yield: 72 mg (45%). ^{1}H NMR (δ, ppm in $CDCl_3$): 8.70 (s, 2 H, −NC*H*N−), 8.08 (s, 2 H, −NC*H*N−), 6.80 (d, 8 H, aromatic C−*H*), 6.64 (m, 24 H, aromatic C−*H*), 6.38 (d, 8 H, aromatic C−*H*), 3.74 (s, 12 H, −CH_3 in DAniF), 3.72 (s, 12 H, −CH_3 in DAniF). UV−vis [λ_{max}, nm (ϵ, M^{-1}·mol^{-1})]: 490 (2.0 × 10^3), 440 (1.1 × 10^3). Anal. Calcd for $C_{74}H_{72}Cl_4Mo_4N_8O_{12}$ (**2**·2CH_2Cl_2): C, 49.62; H, 4.05; N, 6.26. Found: C, 49.52; H, 4.14; N, 6.30.

Preparation of $[Mo_2(cis\text{-}DAniF)_2]_2[(\mu\text{-}o\text{-}O_2C_{10}H_6)_2]$ (3). A procedure similar to that used for the preparation of **2** was employed starting from $[Mo_2(cis\text{-}DAniF)_2(NCCH_3)_4](BF_4)_2$ (208 mg, 0.200 mmol) and 2,3-dihydroxynaphthalene (32 mg, 0.20 mmol). Yield of brown crystals: 80 mg (46%). ^{1}H NMR (δ, ppm in $CDCl_3$): 8.82 (s, 4 H, −NC*H*N−), 7.00 (d, 8 H, aromatic C−*H*), 6.78 (m, 14 H, aromatic C−*H*), 6.50 (m, 14 H, aromatic C−*H*), 6.20 (d, 8 H, aromatic C−*H*), 3.80 (s, 12 H, −CH_3 in DAniF), 3.68 (s, 12 H, −CH_3 in DAniF). UV−vis [λ_{max}, nm (ϵ, M^{-1}·mol^{-1})]: 480 (4.0 × 10^3), 440 (1.8 × 10^3). Anal. Calcd for $C_{81}H_{74}Cl_2Mo_4N_8O_{14}$ (**2**·CH_2Cl_2): C, 52.92; H, 4.06; N, 6.10. Found: C, 52.86; H, 4.14; N, 6.58.

Preparation of $[Mo_2(cis\text{-}DAniF)_2]_2[(\mu\text{-}o\text{-}S_2C_6H_4)_2]$ (4). Benzene-1,2-dithiol (43 mg, 0.30 mmol) was dissolved in 20 mL of ethanol and the solution cooled to 0 °C. This solution was transferred using a cannula to a precooled solution of $[Mo_2(cis\text{-}DAniF)_2(NCCH_3)_4](BF_4)_2$ (208 mg, 0.200 mmol) in 10 mL of ethanol. A brown-orange precipitate formed immediately. The reaction mixture was stirred at 0 °C for 1 h. A treatment similar to that for **2** gave orange needle crystals. Yield: 50 mg (30%). ^{1}H NMR (δ, ppm in $CDCl_3$): 8.26 (s, 4 H, −NC*H*N−), 7.52 (m, 4 H, aromatic C−*H*), 7.12 (m, 4 H, aromatic C−*H*), 6.60 (m, 32 H, aromatic C−*H*), 3.73 (s, 24 H, −CH_3). UV−vis [λ_{max}, nm (ϵ, M^{-1}·mol^{-1})]: 645 (1.0 × 10^3), 455 (8.0 × 10^3). Anal. Calcd for $C_{73.5}H_{71}Cl_3S_4Mo_4N_8O_8$ (**2**·1.5CH_2Cl_2): C, 48.69; H, 3.94; N, 6.18. Found: C, 48.42; H, 3.75; N, 6.18.

X-ray Structure Determinations. A single-crystal suitable for X-ray diffraction analysis for each of the compounds was mounted and centered in the goniometer of a Bruker SMART 1000 CCD area detector diffractometer and cooled to −60 °C. Cell parameters were determined using the program *SMART*.[18] Data reduction and integration were performed with the software package *SAINT*,[19] and absorption corrections were applied using the program *SADABS*.[20] In all structures, the positions of the heavy atoms were found via

(17) Chisholm, M. H.; Cotton, F. A.; Daniels, L. M.; Folting, K.; Huffman, J. C.; Iyer, S. S.; Lin, C.; Macintosh, A. M.; Murillo, C. A. *J. Chem. Soc., Dalton Trans.* **1999**, 1387.

(18) *SMART: Software for the CCD Detector System*, version 5.05; Bruker Analytical X-ray System, Inc.: Madison, WI, 1998.

(19) *SAINT: Data Reduction Software*, version 6.36A; Bruker Analytical X-ray System, Inc.: Madison, WI, 2002.

(20) *SADABS: Bruker/Siemens Area Detector Absorption and Other Corrections*, version 2.03; Bruker Analytical X-ray System, Inc.: Madison, WI, 2002.

direct methods using the program *SHELXTL*.[21] Subsequent cycles of least-squares refinement followed by difference Fourier syntheses revealed positions for the remaining non-H atoms. H atoms were added in idealized positions. Non-H atoms were refined with anisotropic displacement parameters. Some of the anisyl groups in the DAniF ligands in **2** and **3** and interstitial CH_2Cl_2 molecules were found to be disordered and were refined with soft constraints.

Computational Details. DFT[22] calculations were performed with the hybrid Becke's[23] three-parameter exchange functional and the Lee−Yang−Parr[24] nonlocal correlation functional (B3LYP) in the *Gaussian 03* program.[25] Double-ζ-quality basis sets (D95)[26] were used for C, N, and H atoms as implemented in Gaussian. For O and S atoms, correlation-consistent double-ζ basis sets (CC-PVDZ)[27] were applied. The CC-PVDZ includes as the default 3d orbitals on O and 3d and 4d orbitals for S. A small effective core potential representing the 1s2s2p3s3p3d core was used for Mo atoms along with its corresponding double-ζ basis set (LANL2DZ).[28] All calculations were performed on either an Origin 3800 64-processor SGI or an Origin 2000 32-processor SGI supercomputer located at the Texas A&M University supercomputing facility.

Results and Discussion

Syntheses. Compounds **2**−**4** were prepared by mixing the Mo_2 starting material $[Mo_2(cis\text{-DAniF})_2(NCCH_3)_4](BF_4)_2$ with the appropriate linker using a procedure similar to that for the syntheses of halide[13,14] and alkoxide-bridged compounds.[15] Compared to the early approach to these types of Mo_2 pairs,[9] this method is straightforward and convenient, and the yields are generally good. However, small modifications are usually necessary depending on the nature of the linker. For the preparation of halide and alkoxide-bridged compounds, commercially available tetrabutylammonium halides and sodium methoxide were used. Here, the corresponding neutral ligand, not a salt, was used for the assembly reaction with the Mo_2^{4+} precursor, as shown in eq 1.

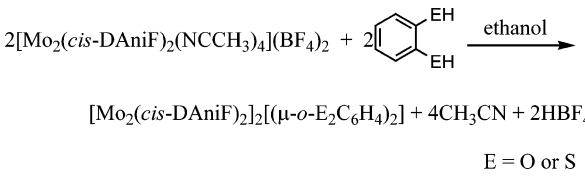

(1)

Because the $o\text{-}C_6H_4(EH)_2$ reactants are fairly acidic, spontaneous deprotonation occurs as complexation takes place at room temperature. A polar solvent, e.g., ethanol, is used to provide an additional driving force because of the low solubility of the neutral products in such solvents. It should be mentioned that it is very important to stay away from basic conditions to avoid hydroxide- and alkoxide-bridged impurities. The synthesis of **4** was carried out at low temperature because benzene-1,2-dithiol was found to be far more reactive than pyrocatechol.

Compound **1** was synthesized differently because reaction of NaOH with the Mo_2 starting material in an organic solvent did not afford the target compound. In earlier work, we noticed that alkoxide-bridged compounds were partially hydrolyzed if the solvents were not freshly dried. This facile hydrolysis was used as an advantage for the preparation of **1** in a reaction carried out in situ. After the addition of sodium methoxide to the Mo_2 corner species to generate the methoxide-bridged compound $[Mo_2]_2(\mu\text{-OMe})_4$,[15,29] subsequent hydrolysis conveniently afforded the crystalline product.

Structural Results. X-ray crystallographic data for compounds **1**−**4** are listed in Table 1, and selected bond distances and angles, along with the structural parameters for other known type **III** compounds, are given in Table 2. The structure of the core for **1**, shown in Figure 1, resembles that in other Mo_4X_4 cuboidal clusters and is closely related to those in the alkoxo analogues $[Mo_2(cis\text{-DAniF})_2]_2(\mu\text{-OR})_4$ (R = Me, Et).[15] In **1**, there are two crystallographically independent but structurally similar molecules in the unit cell. Both of these molecules reside on an inversion center. The nonbonding separation between the two Mo_2 units of 3.23 Å is similar to that of the methoxide bridged analogue (3.24 Å). The crystallographically independent Mo−Mo distances for the two molecules, 2.111(1) and 2.113(1) Å, resemble those in $[Mo_2(cis\text{-DAniF})_2]_2(\mu\text{-X})_4$ but are noticeably shorter than the metal−metal bonds in the analogous OR-bridged species (ca. 2.132 Å). This can be attributed to the lower basicity of the OH groups compared to that of the OR groups that donate more electron density to the metal center.

As shown in Scheme 3, for **2** and **3**, one could envision the formation of two possible geometric isomers having an idealized $[Mo_2]_2(\mu\text{-O})_4$ cuboidal core. In structure **A**, the two O atoms from each of the bidentate anions bind to all four Mo atoms in such a way that the C−C bond in the O−C−

(21) Sheldrick, G. M. *SHELXTL*, version 6.12; Bruker Analytical X-ray Systems, Inc.: Madison, WI, 2000.
(22) (a) Hohenberg, P.; Kohn, W. *Phys. Rev. B* **1964**, *136*, B864. (b) Parr, R. G.; Yang, W. *Density Functional Theory of Atoms and Molecules*; Oxford University Press: Oxford, U.K., 1989.
(23) (a) Becke, A. D. *Phys. Rev. A* **1988**, *38*, 3098. (b) Becke, A. D. *J. Chem. Phys.* **1993**, *98*, 1372. (c) Becke, A. D. *J. Chem. Phys.* **1993**, *98*, 5648.
(24) Lee, C. T.; Yang, W. T.; Parr, R. G. *Phys. Rev. B* **1998**, *37*, 785.
(25) Frisch, M. J.; Trucks, G. W.; Schlegel, H. B.; Scuseria, G. E.; Robb, M. A.; Cheeseman, J. R.; Montgomery, J. A., Jr.; Vreven, T.; Kudin, K. N.; Burant, J. C.; Millam, J. M.; Iyengar, S. S.; Tomasi, J.; Barone, V.; Mennucci, B.; Cossi, M.; Scalmani, G.; Rega, N.; Petersson, G. A.; Nakatsuji, H.; Hada, M.; Ehara, M.; Toyota, K.; Fukuda, R.; Hasegawa, J.; Ishida, M.; Nakajima, T.; Honda, Y.; Kitao, O.; Nakai, H.; Klene, M.; Li, X.; Knox, J. E.; Hratchian, H. P.; Cross, J. B.; Bakken, V.; Adamo, C.; Jaramillo, J.; Gomperts, R.; Stratmann, R. E.; Yazyev, O.; Austin, A. J.; Cammi, R.; Pomelli, C.; Ochterski, J. W.; Ayala, P. Y.; Morokuma, K.; Voth, G. A.; Salvador, P.; Dannenberg, J. J.; Zakrzewski, V. G.; Dapprich, S.; Daniels, A. D.; Strain, M. C.; Farkas, O.; Malick, D. K.; Rabuck, A. D.; Raghavachari, K.; Foresman, J. B.; Ortiz, J. V.; Cui, Q.; Baboul, A. G.; Clifford, S.; Cioslowski, J.; Stefanov, B. B.; Liu, G.; Liashenko, A.; Piskorz, P.; Komaromi, I.; Martin, R. L.; Fox, D. J.; Keith, T.; Al-Laham, M. A.; Peng, C. Y.; Nanayakkara, A.; Challacombe, M.; Gill, P. M. W.; Johnson, B.; Chen, W.; Wong, M. W.; Gonzalez, C.; Pople, J. A. *Gaussian 03*, revision C.02; Gaussian, Inc.: Wallingford, CT, 2004.
(26) (a) Dunning, T. H.; Hay, P. J. Modern Theoretical Chemistry. In *Methods of Electronic Structure Theory*; Schaefer, H. F., III, Ed.; Plenum Press: New York, 1977; Vol. 3, pp 1−28. (b) Woon, D. E.; Dunning, T. H. *J. Chem. Phys.* **1993**, *98*, 1358.
(27) (a) Dunning, T. H. *J. Chem. Phys.* **1989**, *90*, 1007. (b) Woon, D. E.; Dunning, T. H. *J. Chem. Phys.* **1993**, *98*, 1358. (c) Wilson, A. K.; Woon, D. E.; Peterson, K. A.; Dunning, T. H. *J. Chem. Phys.* **1999**, *110*, 7667.
(28) (a) Wadt, W. R.; Hay, P. J. *J. Chem. Phys.* **1985**, *82*, 284. (b) Hay, P. J.; Wadt, W. R. *J. Chem. Phys.* **1985**, *82*, 299.

(29) $[Mo_2]$ is used as an abbreviation for the $[Mo_2(cis\text{-DAniF})_2]$ unit.

Table 1. X-ray Crystallographic Data

compound	**1**·2THF	**2**·0.5CH_2Cl_2	**3**·CH_2Cl_2	**4**·2CH_2Cl_2
empirical formula	$C_{68}H_{80}Mo_4N_8O_{14}$	$C_{73}H_{70}ClMo_4N_8O_{12}$	$C_{81}H_{74}Cl_2Mo_4N_8O_{12}$	$C_{74}H_{72}Cl_2Mo_4N_8O_8S_4$
fw	1617.16	1706.03	1806.14	1855.20
space group	$P\bar{1}$ (No. 2)	$P\bar{1}$ (No. 2)	$P\bar{1}$ (No. 2)	$P\bar{1}$ (No. 2)
a, Å	12.740(4)	10.590(3)	10.480(6)	10.365(4)
b, Å	12.859(4)	14.603(4)	14.735(8)	15.036(5)
c, Å	20.917(6)	14.675(4)	14.792(8)	15.210(5)
α, deg	94.484(5)	104.881(5)	104.701(9)	118.909(6)
β, deg	91.957(6)	108.272(4)	105.451(9)	94.175(6)
γ, deg	95.536(5)	106.460(5)	109.507(8)	103.173(6)
V, Å^3	3397(2)	1912(1)	1922(2)	1973(1)
Z	2	1	1	1
T, K	213	213	213	213
λ, Å	0.710 73	0.710 73	0.710 73	0.710 73
d_{calcd}, g·cm^{-3}	1.581	1.482	1.560	1.561
μ, mm^{-1}	0.791	0.773	0.774	0.920
R1[a] (wR2[b])	0.1044 (0.1124)	0.0664 (0.1649)	0.0786 (0.1845)	0.1449 (0.1943)

[a] $R1 = \sum|F_o| - |F_c|/\sum|F_o|$. [b] $wR2 = [\sum[w(F_o^2 - F_c^2)^2]/\sum[w(F_o^2)^2]]^{1/2}$.

Table 2. Selected Bond Distances (Å) and Angles (deg) for $[Mo_2]_2(\mu\text{-}X_4)$ Cuboidal Clusters

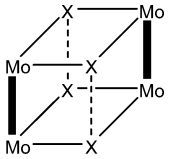

bridge (X)	Mo−Mo	$Mo_2\cdots Mo_2$	Mo−X	Mo−X−Mo	X−Mo−X	X···X (diagonal)	X···X (edge)	ref
Cl	2.1191(4)	3.601	2.516[2]	91.42[5]	81.06[4]	3.273	3.419	13
Br	2.1181(6)	3.697	2.649[2]	88.50[2]	82.95[3]	3.509	3.564	14
I	2.117(1)	3.915	2.845[2]	87.02[2]	86.43[3]	3.802	3.768	14
OMe	2.1315(7)	3.245	2.142[4]	98.6[2]	74.4[2]	2.570	3.206	15
OEt	2.1317(4)	3.241	2.136[2]	98.67[9]	74.1[1]	2.575	3.190	15
OH (**1**)	2.112[2]	3.254	2.127[7]	100.0[3]	74.9[2]	2.581	3.093	this work
O_2 (**2**)	2.1135[9]	3.266	2.137[5]	99.8[2]	75.2[2]	2.605	2.999	this work
O_2 (**3**)	2.113[1]	3.290	2.150[7]	99.9[2]	75.4[2]	2.629	2.977	this work
S_2 (**4**)	2.093[2]	3.724	2.527[5]	95.1[1]	77.7[1]	3.166	3.350	this work

C−O unit is essentially parallel to the two Mo_2 units, while in structure **B**, the O atoms from each linker bind to only two Mo atoms. As shown in Figure 2, the structure of **2**, from crystals that formed in the space group $P\bar{1}$, with the molecule residing on a special position, adopts a type **A** structure. A similar structure is adopted by **3**.[30]

When the structural parameters of **2** (Table 2) are compared to those of **1**, a compound with four isolated bridging OH groups, it is clear that the chelating linkers do not pose significant strain on the core of this complex. The Mo−Mo bond lengths in the two compounds, 2.111(2) Å for **1** and 2.1135(9) Å for **2**, are essentially identical. For both compounds, the Mo_2-Mo_2 nonbonding separations are

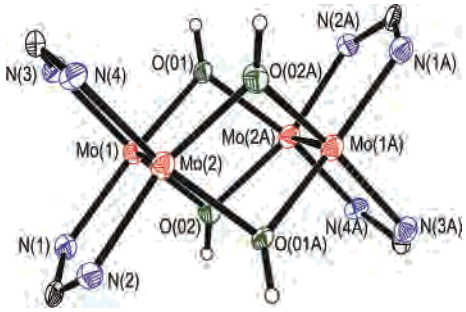

Figure 1. Core structure of one of the crystallographically independent molecules in **1** with displacement ellipsoids drawn at the 40% probability level. All *p*-anisyl groups and H atoms in DAniF have been omitted for clarity.

Scheme 3

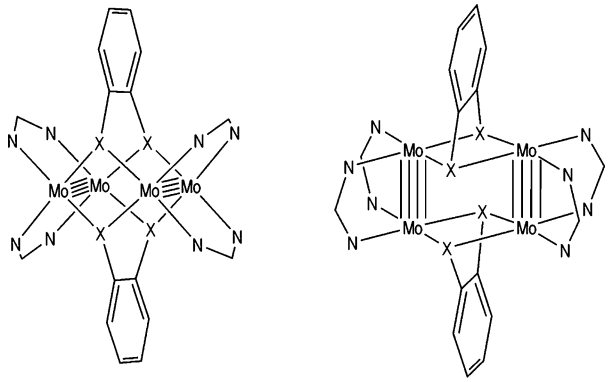

also essentially the same, ca. 3.27 Å. In **2**, the two bridging O atoms in the aromatic ring are separated by 3.02 Å, a separation similar to the corresponding distances between two isolated O-bridging atoms in **1** (ca. 3.09 Å). The O−Mo−O angles in these two compounds are also comparable, that is, 74.8° for **1** and 75.2° for **2**, and the ranges for

(30) A second crystallographic form of **3** was also observed. This form also had a structure of type **A**, but it had significant crystallographic disorder in the linker. Crystallographic data: space group *P*1, *a* = 10.443(4) Å, *b* = 14.887(6) Å, *c* = 23.587(10) Å, α = 87.848(7)°, *β* = 84.995(7)°, *γ* = 87.777(7)°, *V* = 3648(3) Å, *Z* = 2. It should be noted that so far there is no direct evidence for isomers of type **B**.

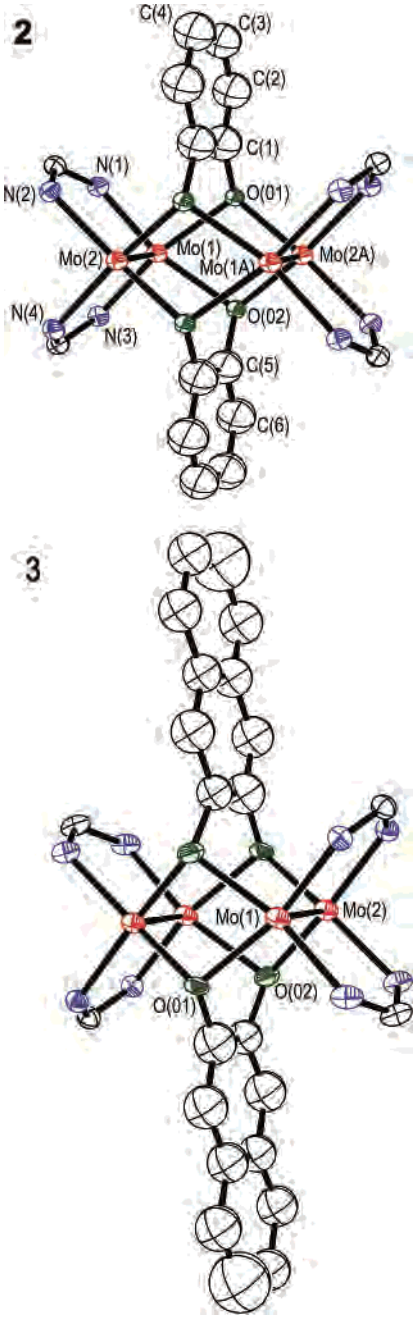

Figure 2. Core structures of **2** and **3** with displacement ellipsoids drawn at the 40% probability level. All *p*-anisyl groups and H atoms have been omitted for clarity.

the Mo−O−Mo angles, 98.9−99.1° for **1** and 99.4−100.1° for **2**, are also similar.

For compound **3**, which has two deprotonated 2,3-dihydroxynaphthalene anions linking two $[Mo_2(cis\text{-}DAniF)_2]^{2+}$ units, the structure is shown at the bottom of Figure 2. Similar to **2**, this compound adopts the type **A** structure. Structural parameters for **3** are generally similar to those in structurally related compounds (Table 2).

Compound **4**, the S analogue of **2**, also crystallized in space group $P\bar{1}$ with $Z = 1$. These two compounds are isostructural, having a type **A** structural motif, as shown in Figure 3. The crystallographically independent Mo−Mo distance, 2.093(2) Å, is significantly shorter than that in **2**

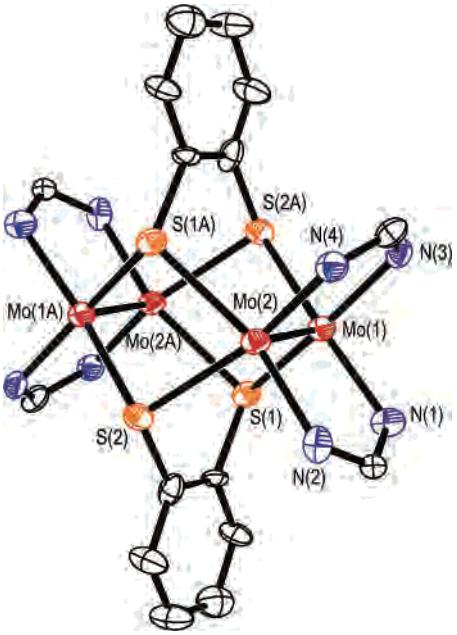

Figure 3. Core structure of **4** with displacement ellipsoids drawn at the 40% probability level. All *p*-anisyl groups and H atoms have been omitted for clarity. Note the structural similarity to the cores of **2** and **3**. However, the $Mo_2\cdots Mo_2$ separation is ca. 0.4 Å longer in **4** than in either **2** or **3**.

by about 0.02 Å (Table 2). This is the Mo_4 cluster with the shortest metal−metal bond. The change in the bridging donor atoms from O to S increases the E−Mo−E angles from 75.3° (E = O) to 77.8° (E = S) but reduces the Mo−E−Mo angles from 99.42−100.03° (E = O) to about 95° (E = S). The $Mo_2\cdots Mo_2$ separation increases by about 0.5 Å from 3.26 to 3.72 Å. For the Mo_4S_4 cuboidal core, the S−S separations along the edges are 3.35 Å and the diagonal S···S separations are 3.17 Å. It should be noted that the many compounds containing M_4S_4 cuboidal cores (M = Mo, W, and Fe) are important in biological systems such as in nitrogenases, but these typically have metal units in tetrahedral environments.[31]

Electrochemistry. Compounds **2**−**4** show two reversible one-electron-oxidation processes.[32] This is shown for the structurally analogous compounds **2** and **4** in Figure 4.[33] The CV of **2** shows the first oxidation process at about 100 mV and the second at about 550 mV (vs Ag/AgCl). These potentials are much more positive than the corresponding values for the alkoxide-bridged compounds, −338 and 216 mV for the methoxide analogue, but the difference in $\Delta E_{1/2}$ for the two types of compounds is relatively small.[34] The shift in the electrochemical potential is attributed to the difference in the Lewis basicity of the bridging ligands

(31) (a) Berlinguette, C. P.; Miyaji, T.; Zhang, Y. G.; Holm, R. H. *Inorg. Chem.* **2006**, *45*, 1997. (b) Rao, P. V.; Holm, R. H. *Chem. Rev.* **2004**, *104*, 527.

(32) Because of the active H atom in each of the hydroxyl bridging groups in **1**, the electrochemical processes are irreversible.

(33) For **3**, there are two sets of signals in the DPV, which appear to be derived from two isomers. For each set (distinguished from each other by the relative intensity), the $\Delta E_{1/2}$ value is the same (450 mV) and similar to that in **2**. Presumably, this is related to the two crystal forms mentioned in ref 30.

(34) Note that there is a strong structural resemblance between **2** and **4** with the alkoxide analogues (see ref 15). For these alkoxides, the singly and doubly oxidized species were isolated and the oxidations were shown to be metal-based processes.

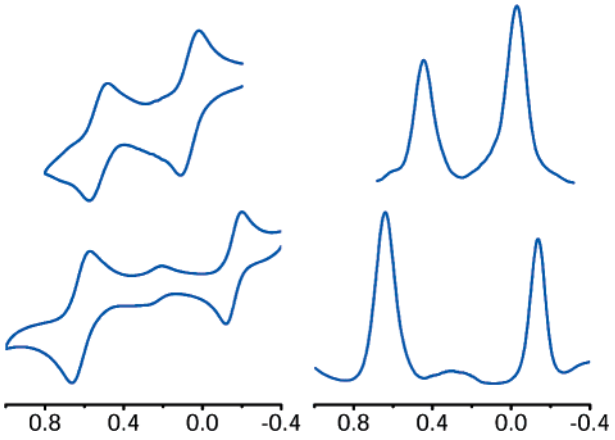

Figure 4. CVs (with potentials vs Ag/AgCl) and DPVs taken in a CH_2Cl_2 solution for the analogous compounds **2** (top) and **4** (bottom), which contain Mo−O and Mo−S bonds, respectively. A small amount of an undetermined impurity is observed in the CV and DPV of **4**. Note the large difference in $\Delta E_{1/2}$ values for these compounds, which is manifested in a K_C value that is 5 orders of magnitude greater for the S-containing compound than for **2**. See the text.

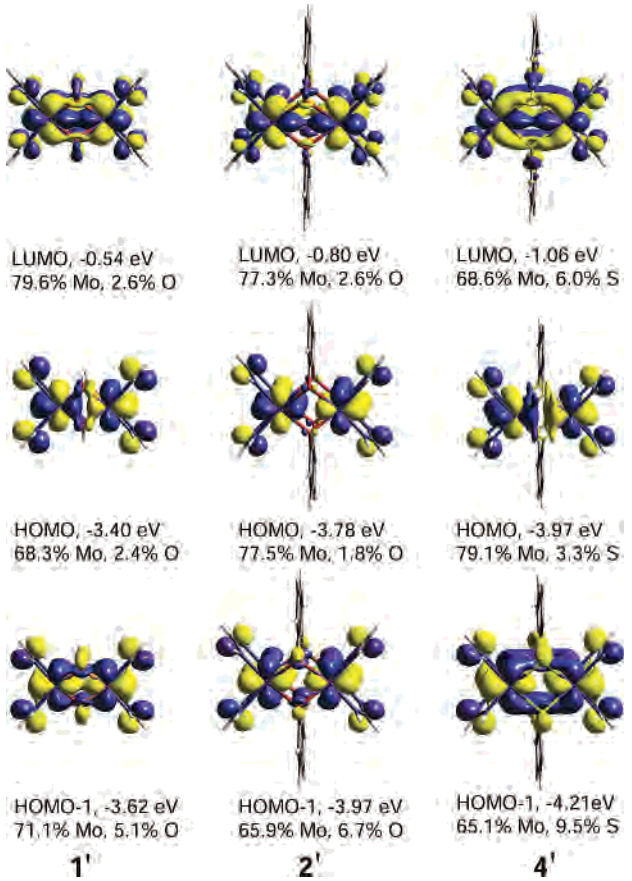

Figure 5. 0.02 surface contour diagrams for the frontier MOs for models **1′**, **2′**, and **4′** calculated using DFT.

because the strongly basic alkoxide anions donate more electron density to the dimetal centers than the diphenol anions. As shown in Table 3, the electrochemical oxidations for $[Mo_2(cis\text{-}DAniF)_2]_2(\mu\text{-}Cl_4)$, which occur at 260 and 800 mV, are shifted by more than 100 mV when compared to **2**, but again these compounds have similar $\Delta E_{1/2}$ values. This is because halides are much weaker Lewis bases than the bidentate ligands reported here.

Compound **4**, the first $[Mo_2]_2(\mu\text{-}S_4)$ cluster, has an $E_{1/2}(1)$ value that is considerably more negative than that in **2**, but $E_{1/2}(2)$ is more positive. However, the most striking difference is the $\Delta E_{1/2}$ value of 776 mV, which is significantly larger than the $\Delta E_{1/2}$ values for any other Mo_4 cluster (see Table 3). The large potential separation is suggestive of large electronic communication, and this occurs despite the increase in the nonbonding separation between the midpoints of the Mo_2 units, which changes from 3.266 Å in **2** to 3.72 Å in **4**, and the increase of ca. 0.4 Å in M−E distances, E = O and S. Both of the latter factors would be expected to diminish the degree of communication between the dimetal units because partial bond formation using the δ-type molecular orbitals (MOs) would be disfavored. Thus, the electrochemical behavior of **4** does not follow the linear relationship of $\Delta E_{1/2}$ vs metal-to-metal separation found for the series of compounds of the type $[Mo_2]_2(\mu\text{-}X)_4$ (X = Cl, Br, and I).[35] Clearly, the increase in the $\Delta E_{1/2}$ value by more than 300 mV for the S-bridged compound, in which the two Mo_2 groups are farther apart, cannot be interpreted solely by direct metal−metal interaction, and another pathway must be responsible for augmenting the electronic delocalization (vide infra).[36]

Electronic Structure. Calculations at the DFT level were performed on the models $[(HNC(H)NH)_2Mo_2]_2(OH)_4$ (**1′**), $[(HNC(H)NH)_2Mo_2]_2(O_2C_6H_4)_2$ (**2′**), and $[(HNC(H)NH)_2Mo_2]_2(S_2C_6H_4)_2$ (**4′**), in which the aryl groups in the formamidinate groups were replaced by H atoms, a simplification that has been used successfully in calculations for compounds with $Mo_2(DAniF)_3$ or $cis\text{-}Mo_2(DAniF)_2$ units linked by various bridges.[8,14] The calculated energies and selected geometries for the models **1′**, **2′**, and **4′** are listed in Table 4.

Because of the idealized D_{2h} symmetry of the Mo_4 clusters, the frontier MOs are formed mainly through the δ-orbital interactions between the two dimetal units (Scheme 2). In-phase and out-of-phase combinations of the δ-antibonding orbitals generate the LUMO ($\delta^* + \delta^*$) and LUMO + 1 ($\delta^* - \delta^*$), respectively, while the HOMO − 1 and HOMO are composed of $\delta + \delta$ and $\delta - \delta$ combinations (Figure 5). The magnitude of the energy difference (ΔE) between the HOMO − 1 and HOMO reflects, to some extent, the strength of the orbital interactions, and it has been used to assess the degree of metal−metal coupling. It is expected that a large calculated energy gap (ΔE from the DFT calculations) for a strongly electronically coupled system should be reflected in the measured electrochemical $\Delta E_{1/2}$ value. Indeed, this relationship between ΔE (energy) and $\Delta E_{1/2}$ (potential) has been shown to be valid in both strongly and weakly coupled systems having linked Mo_2 units.[8]

(35) For the halide-bridged $[Mo_2]_2(\mu\text{-}X)_4$ compounds, the electronic coupling is affected by direct metal−metal interactions, which may be tuned by controlling the distance between the two dimetal units. For example, the iodide-bridged compound, in which the two Mo_2 centers are separated by 3.915 Å, has a $\Delta E_{1/2}$ of 440 mV, smaller than that for the chloride analogue by 100 mV, because the $Mo_2\cdots Mo_2$ nonbonding distance is reduced to 3.61 Å. See ref 14.

(36) The reader should be cautioned that, because the oxidized species for **4** were not isolated, the second oxidation may have some ligand contribution and may not be entirely metal-based.

Table 3. Oxidation Potentials and Comproportionation Constants for Some $[Mo_2]_2(\mu\text{-}X_4)$ Tetranuclear Compounds

compound	$Mo_2\cdots Mo_2$	$E_{1/2}(1)$	$E_{1/2}(2)$	$\Delta E_{1/2}$	K_C	ref
$[Mo_2(cis\text{-}DAniF)_2]_2(\mu\text{-}Cl)_4$	3.601	260	800	540	1.3×10^9	13
$[Mo_2(cis\text{-}DAniF)_2]_2(\mu\text{-}Br)_4$	3.697	314	813	499	2.7×10^8	14
$[Mo_2(cis\text{-}DAniF)_2]_2(\mu\text{-}I)_4$	3.915	350	790	440	2.7×10^7	14
$[Mo_2(cis\text{-}DAniF)_2]_2(\mu\text{-}OMe)_4$	3.245	−338	216	554	2.3×10^9	15
$[Mo_2(cis\text{-}DAniF)_2]_2(\mu\text{-}OEt)_4$	3.241	−418	169	587	8.4×10^9	15
$[Mo_2(cis\text{-}DAniF)_2]_2(\mu\text{-}O_2C_6H_4)_2$	3.266	75	529	474	1.0×10^8	this work
$[Mo_2(cis\text{-}DAniF)_2]_2(\mu\text{-}S_2C_6H_4)_2$	3.724	−155	621	776	1.3×10^{13}	this work

Table 4. Calculated Data from DFT for Models **1′**, **2′**, and **4′**

					calculated bond lengths (Å) and angles (deg)			
model	energy (au)	HOMO (eV)	HOMO − 1 (eV)	ΔE (eV)	Mo−Mo	$Mo_2\cdots Mo_2$	Mo−L	Mo−L−Mo
1′	−1171.4486	−3.40	−3.62	0.22	2.168	3.348	2.173	100.79
2′	−1631.0351	−3.78	−3.97	0.19	2.144	3.435	2.214	101.76
4′	−2923.0042	−3.97	−4.21	0.24	2.143	3.861	2.600	95.92

The calculations on the models **2′** and **4′** (Figure 5 and Table 4) show the difference in the electronic structure between the O- and S-linked species. The calculated energy gap (ΔE) between the HOMO and HOMO − 1 of 0.24 eV for the model **4′** is larger than 0.19 eV for the model **2′**. This is consistent with the electrochemical data that show a larger redox potential separation for **4** than for **2**. Recent DFT calculations on the *dimers of dimers* $[(HCO_2)_3M_2]_2(p\text{-}X{-}C_6H_4{-}X)$ (M = Mo and W and X = CO_2, COS, and CS_2) revealed that successive substitution of O by S also leads to enhanced electronic coupling in such systems as evidenced by the increased energy separation of the HOMO and HOMO − 1.[16a] This has also been observed in $[Mo_2]L[Mo_2]$ compounds when the unsubstituted oxamidate linker L was replaced by the corresponding dithiooxamidate linker.[16b]

In the *dimers of dimers* $[(HCO_2)_3M_2]_2(p\text{-}X{-}C_6H_4{-}X)$ (X = CO_2, COS, and CS_2) and dithiooxamidate-bridged species, which have only one linker joining the two Mo_2 units, the enhanced coupling arises principally from a lowering of the π^* orbital of the linkers as the E donor atoms change from O to S.[16] However, for the tetranuclear clusters $[Mo_2]_2(\mu\text{-}E{-}E)_2$, in which the Mo_2 units are joined by two linkers, the LUMO and LUMO + 1 are both metal-based orbitals and the linker-based π^* orbital is higher in energy and thus is not accessible for electronic coupling. Therefore, an alternative pathway must be responsible for the large increase in electronic communication in **4**. As is often recognized, an important difference between S and O compounds is that the S d orbitals are available for additional bonding interactions and S atoms frequently use $d{-}\pi$ interactions to form multiple bonds. For example, in the sulfate ion, the S−O bonds have considerable multiple-bond character, as evidenced by the shortness of the bond distance.[37] In the sulfate ion, the empty $d\pi$ orbitals of the S atom accept electrons from the $p\pi$ orbitals of the O atoms. Similarly, here the $d\pi$ orbitals of the S atoms in the linkers can accept electrons from the δ orbitals of the dimetal units, providing an electron pathway that has some $d\pi{-}d\delta$ character (Scheme 4, the view along the Mo_2 axes).[38] Indeed the coefficients for d orbitals

Scheme 4

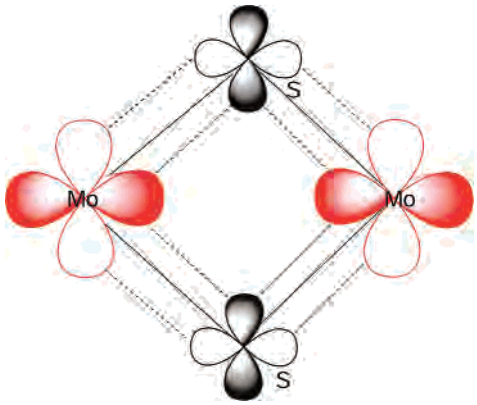

Scheme 5

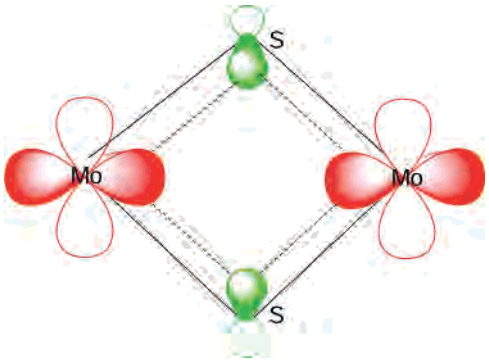

for the HOMO − 1 and LUMO for **2′** and **4′**, although small, are significantly larger for the S linker than for the O linker, as shown in Figure 5 and the Supporting Information.

To a lesser extent, the filled S p orbitals also contribute to the mixing with the metal $d\delta$ orbitals, as shown by the MO diagram (viewed along the Mo_2 axes) in Scheme 5. When O serves as the bridge in **2′**, the LUMO is composed of 2.6% O and the HOMO − 1 of 6.7% O. However, in the S-containing model **4′**, S contributes 6.0 and 9.5%, respectively, to the LUMO and HOMO − 1.[39]

These two pathways are less important for **2**, for which the electronic communication occurs mainly through direct interaction between δ orbitals, as in $[Mo_2]_2(\mu\text{-}X)_4$ and $[Mo_2]_2$-

(37) Cotton, F. A.; Wilkinson, G.; Murillo, C. A.; Bochmann, M. *Advanced Inorganic Chemistry*, 6th ed.; John Wiley & Sons, Inc.: New York, 1999.

(38) It should be noted that the donation of electrons in the δ orbitals is unique to compounds with quadruply bonded units.

(μ-OR)$_4$ compounds.[14,15] This is also different from what is observed in *dimers of dimers* containing one linker with S- and O-donor atoms, where an "electron-hopping" pathway from the metal δ to bridge π^* orbital has been suggested.[16] In spite of the difference in the pathway, the principal reason for the increase in electronic communication in both types of compounds is the lowering of the orbital energy for S-donor linkers relative to the corresponding O-donor ligands.

Conclusions

In this work, a tetranuclear cluster containing two quadruply bonded Mo_2 units linked by four hydroxide groups (**1**) and analogues linked by two bidentate bridges (*o*-$O_2C_6H_4$ for **2**, *o*-$O_2C_{10}H_6$ for **3**, and *o*-$S_2C_6H_4$ for **4**) were synthesized from corner species $[Mo_2(cis\text{-DAniF})_2(NCCH_3)_4](BF_4)_2$ and the corresponding linker. The Mo−S distances in **4** are ca. 0.4 Å longer than those of the Mo−O bonds in **1**−**3**, and consequently the nonbonding separation between the midpoints of the Mo_2 units changes from 3.27 Å in **1**−**3** to 3.72 Å in **4**. In spite of the lengthening of the $[Mo_2]\cdots[Mo_2]$ separation, electronic coupling between the two Mo_2 units was enhanced by replacement of the O atoms by S atoms, as evidenced by electrochemical measurements, which show two reversible one-electron-oxidation processes with potential separations ($\Delta E_{1/2}$) between the two oxidation processes of 474 and 776 mV, respectively. DFT calculations suggest that the enhancement in electronic communication between the metal centers in **4** can be attributed to two factors: (1) the mixing of metal δ orbitals with empty S dπ orbitals (Scheme 4) and (2) the increase of filled S p orbitals with the metal (Scheme 5). This is different from the *dimers of dimers* joined by only one linker[16] in which a low-energy π^* orbital of the S-containing linker facilitates an electron-hopping pathway.

Acknowledgment. We thank the Robert A. Welch Foundation, the National Science Foundation (IR/D support), and Texas A&M University for financial support.

Supporting Information Available: X-ray crystallographic data for **1**·2THF, **2**·0.5CH_2Cl_2, **3**, and **4**·CH_2Cl_2 in standard CIF format and a table of coefficients for selected atomic orbitals in frontier MOs for **2′** and **4′** from DFT calculations as well as input files for DFT calculations for **2′** and **4′** in PDF format. This material is available free of charge via the Internet at http://pubs.acs.org.

IC701303K

(39) It should be noted that the effect of the difference in orbital composition on the electronic coupling is even larger than what the absolute numbers reflect. The orbitals involved in electronic coupling are $2p_z$ for O atoms and $3p_z$ and $3d_{xy}$ for S atoms (Schemes 4 and 5). In both cases, the corresponding contributions from S are greater than those from O for the HOMO − 1 and LUMO (see the Supporting Information).